Development and geometry of isotropic and directional shrinkage-crack patterns

Kelly A. Shorlin* and John R. de Bruyn
Department of Physics and Physical Oceanography, Memorial University of Newfoundland, St. John's, Newfoundland, Canada A1B 3X7

Malcolm Graham and Stephen W. Morris
Department of Physics, University of Toronto, 60 St. George Street, Toronto, Ontario, Canada M5S 1A7
(Received 11 November 1999)

We have studied shrinkage-crack patterns which form when a thin layer of an alumina/water slurry dries. Both isotropic and directional drying were studied. The dynamics of the pattern formation process and the geometric properties of the isotropic crack patterns are similar to what is expected from recent models, assuming weak disorder. There is some evidence of a gradual increase in disorder as the drying layer become thinner, but no sudden transition, in contrast to what has been seen in previous experiments. The morphology of the crack patterns is influenced by drying gradients and front propagation effects, with sharp gradients having a strong orienting and ordering effect.

PACS number(s): 62.20.Mk, 46.50.+a, 81.40.Np, 45.70.Qj

I. INTRODUCTION

Shrinkage-crack patterns are common in both natural and manmade systems [1], including dried mud layers and the glaze on a ceramic mug. They are in many instances undesirable, as in the case of paint or other protective coatings. Crack patterns have long been of interest in geology, in connection with the formation of columnar joints [2,3] and ancient crack patterns preserved in the geological record [4,5]. They arise in materials which contract on cooling or drying. This contraction, coupled with adhesion to a substrate, leads to a buildup of stress in the material, and when the stress exceeds the local tensile strength, the material fractures. This relieves the stress locally along the sides of the crack, but concentrates stress at the crack tip. As a result the crack tip propagates until the stress there is reduced below the local strength of the material [6]. A crack pattern forms as multiple cracks grow and interconnect. In a homogeneous medium a crack will form, and grow perpendicularly to the direction of maximum stress. Since the stress near an existing crack face is parallel to the face, any crack nucleating at or growing to meet the edge of a preexisting crack will meet that crack perpendicularly. Nonperpendicular junctions can form due to the influence of nearby cracks on the local stress field, by the nucleation of multiple cracks at a point, or by the splitting of a crack tip into multiple cracks. The lateral length scales of crack patterns range from millimeters in thin layers of ceramic glaze to tens of meters in the case of ice-wedge polygons found in the Arctic [7].

Shrinkage results from the removal of a diffusing quantity—water in the case of dessication, or heat in the case of cooling. In thin layers, crack development can be slow enough compared to diffusion in that the layer is homogeneous over its thickness and the resulting crack pattern is effectively two dimensional. In contrast, in the drying or cooling of thick layers, gradients of the diffusing quantity—which can only be removed from exterior surfaces—become important. Cracks tend to propagate in the direction of the gradient, following it as it moves through the material. This leads to three-dimensional crack patterns. The crack pattern in turn affects the rate of removal of the diffusing quantity. Remarkably, an initially disordered network can become more ordered as it propagates into the material. This leads, for example, to the formation of hexagonal columnar joints in cooling basaltic lavas [2,3]. This ordering process is currently poorly understood [2,3].

In this paper we report on experiments on crack patterns formed by the drying of slurries of 130 Å alumina (Al_2O_3) particles [8] in water. We study two-dimensional patterns formed in a uniformly dried thin layer. A typical crack pattern formed in one of these experiments in shown in Fig. 1. We also performed experiments on ''directional drying'' [9], in which a one-dimensional pattern of cracks propagates due to a moving drying front. A pattern formed by directional drying is shown in Fig. 2.

Although qualitative observations of crack patterns were reported several decades ago [4,5], there have been rather few well-controlled experimental studies of the phenomenon. Skejltorp and Meakin [10] investigated the drying of monolayers of close-packed polystyrene beads. Cracks formed at grain boundaries, and propagated in straight lines defined by the hexagonal lattice of the beads. Later cracks were wavy. Groisman and Kaplan [11] studied crack patterns in layers of coffee-water mixtures. They found that the length scale of the pattern was proportional to the layer thickness d, and increased when the bottom friction was reduced. For thick layers they observed a polygonal pattern consisting mostly of straight cracks meeting at 90° junctions. As d decreased, they observed a transition below which a large fraction of the junctions were at 120°, and wavy cracks appeared. A similar transition was observed in drying corn flour-water mixtures by Webb and Beddoe [12]. Pauchard *et al.* [13] studied the dessication of colloidal silica sols; in this case the fluid properties are complex, and the nature of the crack patterns was a function of the ionic strength of the suspension. Korneta *et al.* [14] studied the geometrical properties of shrinkage-

*Present address: Department of Physics, University of Western Ontario, London ON, Canada.

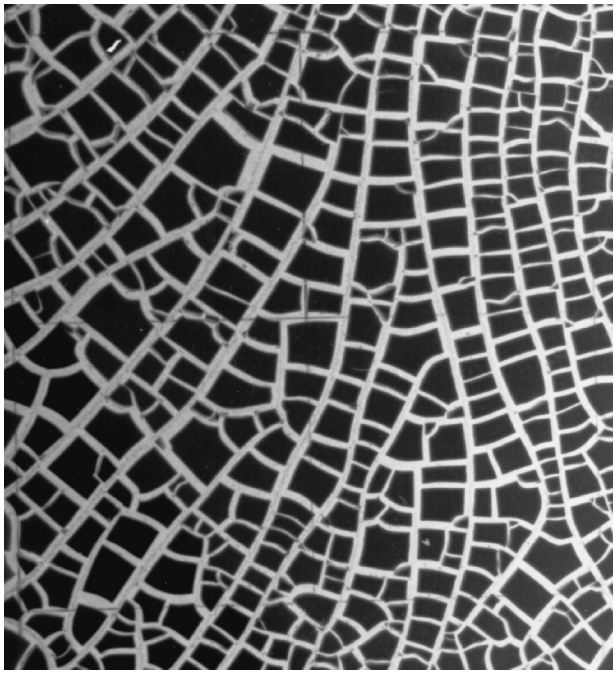

FIG. 1. A portion of the crack pattern formed by drying a 62-cm square layer of an alumina-water mixture. The area shown measures 16.0×16.0 cm^2. The Plexiglas substrate was untreated, and the final thickness of the layer was 2.27 ± 0.20 mm.

crack patterns formed by sudden thermal quenches.

There have been several theoretical and computational studies of two-dimensional crack patterns using spring-block models [10,15–23]. Andersen and co-workers [15–17] observed a transition in the crack-pattern morphology as the strain and the coupling to the substrate were varied. Hornig, Sokolov, and Blumen [20], in a similar model, observed a change in the way in which fragmentation occurred as the amount of disorder in the system was varied: for small disorder, fragments (i.e., polygons) formed through the propagation of cracks in straight lines defined by the lattice structure. Cracks tended to appear in the middle of existing segments, so the length scale of the pattern decreases by a factor of 2 with each generation of cracks. For somewhat larger disorder, cracks propagated along wavy paths. For large disorder, cracks did not propagate, but rather formed by the coalescence of independent point defects. Crosby and Bradley [22] found similar regimes in their simulations, but as a function of the applied stress due to a sudden temperature quench: low stress led to polygonal patterns, and high stress to a complicated pattern of strongly interacting cracks. Recently Kitsunezaki [23] performed theoretical studies of crack-pattern formation, along with numerical simulations using a random two-dimensional lattice, and reproduced many of the qualitative features seen in experiments. Kitsunezaki found analytically that the pattern length scale should be proportional to layer thickness, as observed experimentally, if the fracture occurs due to a critical stress criterion, but would be nonlinear if fracture obeyed the Griffiths criterion [24].

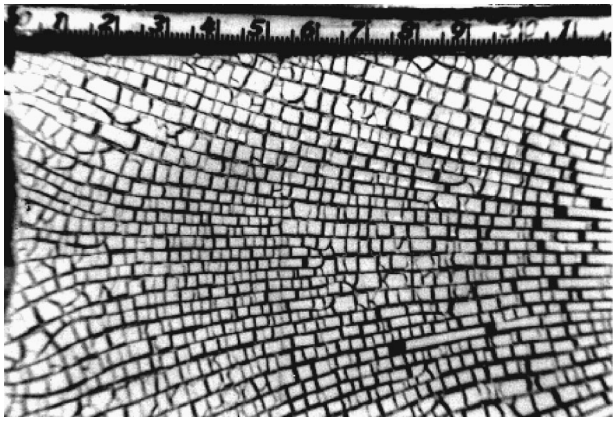

FIG. 2. The crack pattern formed in a directional drying experiment. The substrate was treated with teflon, and a sharp drying front moved front left to right across the layer, leaving behind oriented primary cracks. The rungs of the ladderlike pattern are secondary cracks. The front speed was 1.2 mm/h. Near the middle of the picture, the depth of the layer suddenly increased by about 50%, but no change in the average spacing is evident. This illustrates the weak depth dependence and hysteretic nature of crack spacings on slippery substrates.

There have been fewer studies of directional cracking in the presence of moving gradients in two or three dimensions. Yuse and Sano [25] examined the morphology of *single* cracks which formed in thin glass plates with a moving thermal gradient, and observed an instability of the crack tip as the speed of the cooling front was increased [26]. Fracture patterns in thin layers of a directionally dried colloidal suspension between two glass plates were studied by Allain and Limat [9]. Komatsu and Sasa [27] explained the observed regular crack spacing by again noting that cracks will form in the middle of existing segments where the stress is highest. Their theory [27] predicted a wavelength of the crack pattern that varied as $d^{2/3}$, in good agreement with the experimental results of Ref. [9], but different from the linear relation found for the isotropic case.

Recently Müller studied three-dimensional shrinkage-crack patterns in drying cornstarch-water mixtures [3]. The resulting ''starch columns'' are strikingly similar to basalt columns formed by the cooling of basaltic lava flows. Müller showed that the in-plane length scale of the pattern (i.e., the column width) was dependent on dc/dz, where c is the water concentration at the propagating crack front, and z is the coordinate along the propagation direction. From this he inferred that the column width in basalt is similarly determined by dT/dz, where T is the rock temperature at the crack front.

There has been relatively little theoretical work on three-dimensional gradient problems. Motivated by the experiments of Yuse and Sano [25], Hayakawa [28] considered two- and three-dimensional breakable spring models of directional cracking. In three dimensions, he found columnar structures reminiscent of those found in basalt [2,3], and evidence of scaling behavior in the crack spacing. He did not include adhesion to a substrate, however.

The remainder of this paper is organized as follows. In Sec. II, we describe our experimental apparatus. In Sec. III, we discuss our results, first on the temporal development of uniform and directionally dried crack patterns, and then on the geometric characteristics of the final state. Sections IV and V contain a discussion and a brief conclusion.

II. EXPERIMENT

Shrinkage-crack patterns were produced by drying layers of a slurry of 130-Å Al_2O_3 particles in water. These particles were very uniform, and inspection of the dried layers by eye and with a microscope indicated that the composition of the layers was quite homogeneous over their depth. Two types of experiments were performed: ''isotropic drying,'' in which the entire layer was dried uniformly; and ''directional drying,'' in which the layer was dried from one end.

The mixtures used in the experiments were prepared simply by mixing a weighed quantity of Al_2O_3 particles with a measured volume of water. The isotropic drying experiments were performed by pouring a quantity of the Al_2O_3-water mixture into a Plexiglas pan 62 cm square. The pan was housed in an insulated enclosure. Four 15-W light bulbs mounted 1.6 m above the pan served as a heat source to dry the films, and also provided illumination for video imaging. The temperature of the layer was between 25 and 28 °C for all runs, and was constant to within 1 °C for each run. The humidity of the enclosure was not controlled. Time-lapse video recordings of the cracking process were made using a charge coupled device video camera mounted near the top of the enclosure. Frames from the video record were digitized for later analysis, and photographs of the dried layer taken at the end of each run were also analyzed. Experiments were performed with the Plexiglas substrate untreated, as well as with the substrate coated with a thin transparent coating of teflon to reduce the friction between the drying layer and the substrate. Experiments were also done with the teflon-coated surface, and ''impurities,'' in the form of 10 cm^3 of sand grains, 0.425–0.500 mm in size, sprinkled evenly over the top of the slurry before the drying began. The sand floated on top of the layers during drying. These impurity particles were $\sim 3\times 10^3$ times the size of the alumina particles, and of the same order as the layer thickness. The depth varied somewhat over the 62-cm square layer. The analysis discussed in Sec. III was done on 8-cm square sample areas within the pan away from the edges; the layer depth was uniform to within 5% or better over these smaller regions.

Directional drying experiments were performed on layers of Al_2O_3-water mixture placed in a 12×8-cm^2 rectangular pan. The pan was covered with a sealed window, leaving a 3-mm air space above the layer. A very slow laminar breeze of ultradry N_2 gas, 20° above ambient temperature, was passed unidirectionally through the air space. The N_2 became saturated with water as it passed through the cell, resulting in a drying front that moved downwind. By controlling the rate of flow, the front speed could be varied between 0.01 and 10 mm/h. The progress of the front was monitored with time-lapse video. The roughness of the substrate was varied by putting teflon and various grades of sandpaper on the bottom of the pan. Our apparatus differs from that of Allain and Limat [9], in that here the upper surface of the drying layer is free, and only the lower surface is constrained by adhesion to the substrate. We found that a considerable transport of material occurred over the course of an experiment, so that the final dry layer could be as much as 50% thicker at the downwind end than at the upwind end. This could be compensated for by tilting the apparatus.

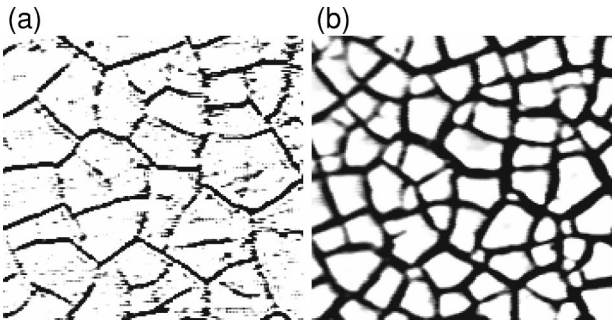

FIG. 3. A portion of the crack pattern forming in a layer 1.31 ± 0.03 mm thick. Sand has been added to the layer, and the substrate coated with teflon. At least five triplet junctions, formed when three cracks nucleated at a point, are visible in the images. The area shown is 5.7×5.5 cm^2. (a) 41 h into the run. (b) 56 h into the run.

III. RESULTS

A. Dynamics

The alumina-water mixture is initially fluid, but becomes gel-like a few hours after being poured into the experimental container. Cracks first appear in the layer after a wait of from several hours to a few days, depending on the thickness and composition of the layer. The drying process in the ''isotropic'' experiments is, of course, neither perfectly isotropic nor perfectly uniform as a result of nonuniformities in thickness and in the heating of the layer by the light bulbs. Because of this, cracks tend to start in one or more separate regions of the layer and move into the rest of the system, so that different parts of the system are at different stages of crack-pattern evolution at any given time. The formation of the crack pattern and complete drying of the layer took up to eight days, again varying with layer thickness.

The dynamics of crack-pattern formation were observed on time-lapse video recordings. Although some characteristic behavior was observed, in some cases paralleling predictions of the theoretical models discussed above, there was no single clearcut path followed during the development of the patterns.

In the first stage of crack-pattern development, cracks nucleate at a small number of points in the layer. In the absence of sand impurities, these cracks then propagate in fairly straight lines, presumably in a direction determined by the local drying conditions. In runs with sand added to the layer, cracks tend to nucleate at the sand grains, and in many cases do not propagate long distances across the layer, but rather move in short steps from one sand grain to the next, occasionally meeting another crack moving in a similar fashion. In runs with no sand, other defects in the layer structure presumably serve as nucleation sites. Typically, symmetric arrangements of two or three cracks nucleate at a site and propagate away from it. Images taken from time-lapse video recordings showing a number of triplets of cracks in the early and later stages of the development of a crack pattern are shown in Fig. 3. More examples can be found in Fig. 4, which shows a pattern from a run in a thin layer with sand impurities. In runs with no sand impurities, the number of these nucleations is small. After the initial nucleation of a few cracks, most new cracks start at the sides of existing cracks, and propagate away from their parent crack at right angles.

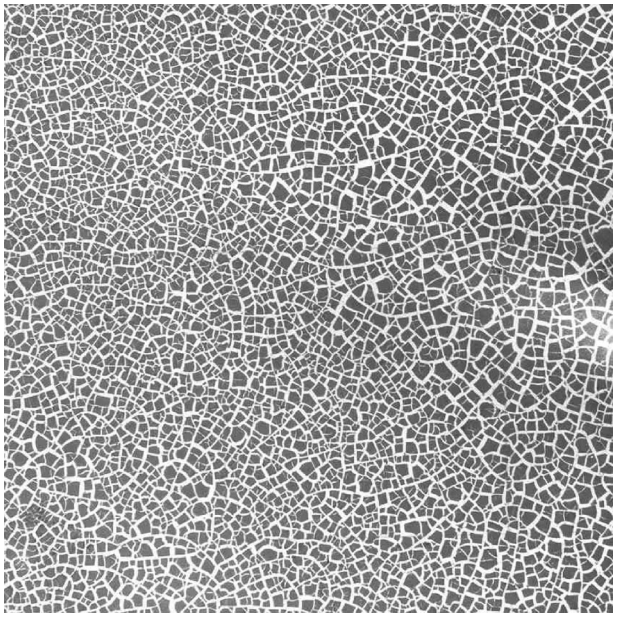

FIG. 4. A portion of the crack pattern formed by drying a 62-cm square layer of an alumina-water mixture. The area shown measures 16.5×16.5 cm^2. The Plexiglas substrate was coated with teflon, and sand was added to the mixture. The final thickness of the layer was 0.60 ± 0.03 mm.

The longest cracks in Fig. 1 are an order of magnitude longer than the final length scale of the pattern. These long, straight cracks are referred to as primary cracks. Although these may not be the very first cracks to form in the layer, they are usually the oldest cracks locally. As the slurry dries further, successive generations of cracks form, often joining older cracks and forming a complicated array of polygons. The resulting pattern has a characteristic length scale, as can be seen in Fig. 1. The polygonal fragments bounded by the cracks are predominantly four sided. Most of the junctions between cracks are at right angles, with a few nonperpendicular junctions. In runs with no sand impurities, the faces of the cracks are smooth and the cracks, while they can curve smoothly, are usually locally straight.

In thinner layers, or layers with sand impurities added, the patterns are more disordered in appearance. An example is shown in Fig. 4. A few long primary cracks are still present, but are much less dominant than in Fig. 1. In runs with sand added, cracks can change direction suddenly, and in thin layers the crack faces appear less smooth. Despite the more disordered appearance of the pattern in Fig. 4, the fragments of dried mud are still predominantly four sided and crack junction angles remain primarily at 90°, as discussed below.

A common process in the isotropic system we call ''arching.'' In this process, a new crack propagates away from an existing pattern of cracks. It then curves back on itself in a roughly parabolic path, eventually stopping as it runs into another crack. The region enclosed by the arch is fragmented by later cracks as it dries further. The stages in this process are illustrated in Fig. 5.

Another very commonly observed mode of pattern formation is shown in Fig. 6; we refer to this process as ''laddering.'' In this process, two or more cracks propagate more or less parallel to each other, following a local drying front. As the layer behind the moving crack tips dries further, perpendicular cracks form, joining two of the parallel cracks like the rungs of a ladder. Figure 6 shows the stages in this process, and regions in which extensive laddering have taken place can be seen in Fig. 1. This process is dominant in the directional drying case, as can be seen in Fig. 2, and clearly involves a local directionality of the drying process in an essential way.

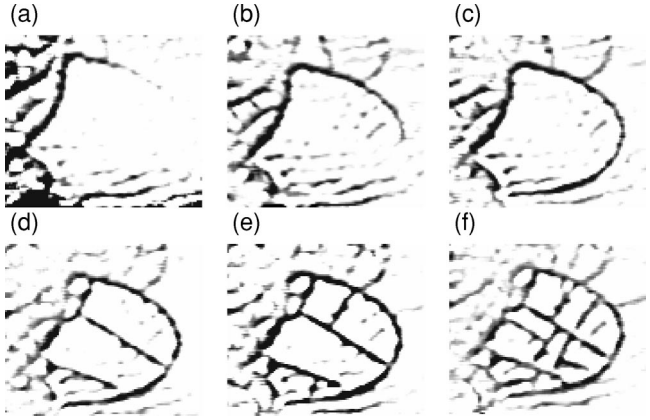

FIG. 5. A sequence of images of a portion of a crack pattern forming in a layer of final depth 1.51 ± 0.06 mm with a teflon coated substrate. The field of view is 5.1×4.8 cm^2. Image (a) is 33 h after the start of the run, and the elapsed time between (a) and (f) is 6 h. This sequence illustrates the ''arching'' process described in the text.

Using the directional drying technique, we could examine the laddering process in a more controlled way. The directional experiments involved much sharper fronts than those that emerged spontaneously in the isotropic version of the experiment. Fronts produced alignment, and a uniform spacing similar to that observed by Allain and Limat [9], although on a larger scale. By varying the rate of drying, we found that the spacing of the primary cracks was independent of the speed of front advance over three orders of magnitude. Once the spacing of the primary cracks was established perpendicular to a planar front, we did not observe it to change

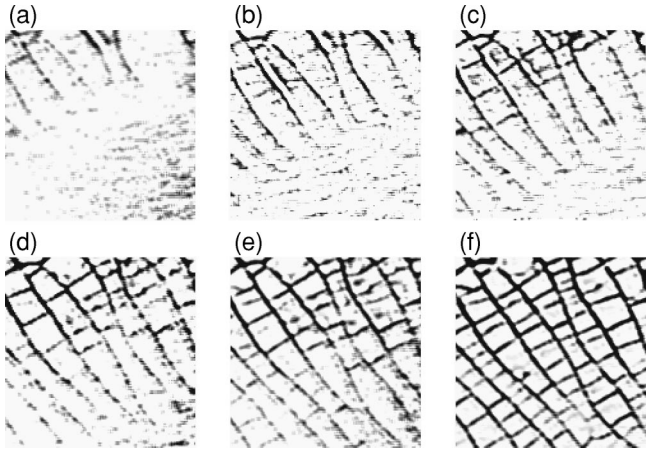

FIG. 6. A sequence of images of a portion of a crack pattern forming in a layer of final depth 1.88 ± 0.10 mm, with an uncoated substrate. The field of view is 7.1 cm square. Image (a) is 67 h after the start of the run, and the elapsed time between (a) and (f) is 17 h. This sequence illustrates the ''laddering'' process described in the text.

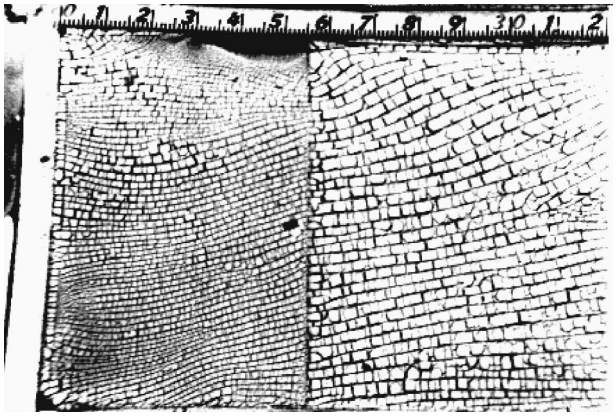

FIG. 7. A directional drying experiment on a rough sandpaper substrate. The sharp drying front moved from left to right across the layer at a speed of 1.5 mm/h. Near the middle of the picture, the depth of the layer suddenly increases by about 50%, as in Fig. 2. At this point, the crack spacing changes abruptly, approximately doubling.

subsequently. In particular, we do not normally observe the sequential bisection proposed in Ref. [27]. The scale of the primary cracks in turn determined that of the secondary, ''rung'' cracks of the ladder.

The primary crack spacing in the directional experiments does not have a simple relationship to the local depth, because the propagation of the front introduces a form of history dependence. We constructed a cell which contained a 0.5-mm downward step, and examined the primary crack pattern as it passed over the step. The subsequent behavior of the primary crack spacing was strongly influenced by the roughness of the substrate. For the teflon-covered substrates, no new primary cracks appeared as the front passed the step, as illustrated in Fig. 2. For substrates covered with the roughest grades of sandpaper, under otherwise identical conditions, the primary crack spacing doubled as it passed over the step, with a primary crack disappearing between each of the original ones. This is shown in Fig. 7. This demonstrates that the primary crack spacing is, in a sense, hysteretic on rough substrates, with a range of spacings which can stably propagate under given conditions.

The theories of Refs. [20] and [27] predict that cracks will tend to form in the middle of existing fragments of the layer, since that is ideally where the stress in the fragment will be largest. In our isotropic experiments new cracks are observed to form at almost any location in an existing fragment. They usually start at one edge, rather than in the interior, and propagate more or less in a straight line across the fragment. It is rare that the new crack will exactly bisect the fragment, presumably due to nonuniformities in the adhesion of the fragment to the substrate or in its dryness or composition. This is evident from the range of sizes of the fragments seen, for example, in Fig. 1. However on occasion, near-perfect bisections do occur; one example is shown in Fig. 8. In this example the regions between propagating parallel cracks are bisected by new cracks, as proposed for the directional drying case in Ref. [27].

In the very late stages of crack-pattern formation, new cracks tend to simply cut off the corners of existing fragments, breaking off a piece much smaller than the original

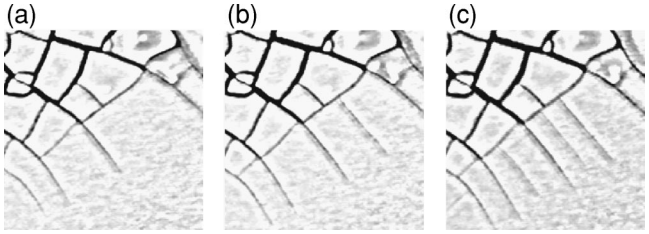

FIG. 8. A sequence of images of a portion of a crack pattern forming in a layer of final depth 2.50 ± 0.14 mm with a teflon coated substrate. The field of view is 9.7 cm square. Image (a) is 135 h after the start of the run, and the elapsed time between (a) and (c) is 5 h. This sequence illustrates the formation of cracks which bisect regions bounded by existing cracks, as predicted in the theory of Ref. [27].

fragment. The results of this process can be seen in many places in Fig. 1.

B. Geometrical characteristics

The characteristic length scale of the final crack pattern was determined in real space, as well as from a Fourier analysis of the patterns. We estimate the pattern ''wavelength'' λ_r by $l/\sqrt{N_p}$ where N_p is the number of polygons in a square region of the pattern of side l. For a perfect pattern of equal-sized squares, this would be equal to the true wavelength. λ_r was measured in a number of 8×8-cm^2 square regions, neglecting the parts of the layer close to the edges, and is plotted as a function of the mean local layer depth d in Fig. 9. In all three sets of isotropic drying experiments (untreated substrate, teflon-coated substrate, and coated substrate plus added impurities) λ_r is proportional to the depth, as found previously by Groisman and Kaplan [11]. The slope is a function of the experimental conditions, with the runs having lower friction between the layer and the substrate [Fig. 9(b)] having the highest slope. Both increased friction

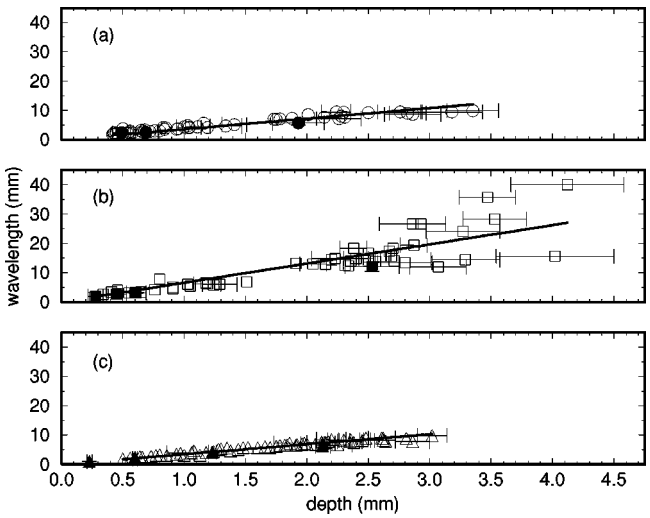

FIG. 9. The pattern wavelength as a function of layer depth for (a) untreated substrate, no impurities; (b) reduced substrate friction, no impurities; and (c) reduced substrate friction with added impurities. Open symbols are values of λ_r, determined geometrically, and solid symbols are values of λ_c, determined from a Fourier analysis of the pattern.

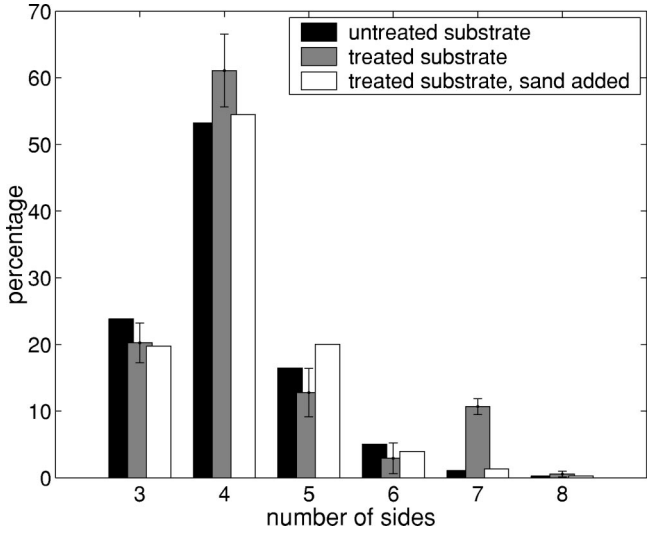

FIG. 10. The distribution of n-sided polygons in the final pattern, averaged over depth, for the three different types of isotropic drying runs. Error bars ($\pm$ one standard deviation) are shown for the treated substrate case; they are similar for the other two cases.

[Fig. 9(a)] and the addition of impurities [Fig. 9(c)] cause the slope to decrease. Equivalently, at a given layer depth, increased friction and the addition of impurities lead to a decrease in the length scale of the pattern. The scatter in the data increases for depths greater than about 2.75 mm, particularly for the runs with reduced friction and no impurities. This may be a result of the decreased effect of bottom friction with thickening layers, or of three-dimensional effects.

The distribution of length scales in the pattern was also studied by performing two-dimensional fast Fourier transforms of video images of the dried layer. This analysis does not require any assumptions about the shape or orientation of the polygons making up the pattern. The two-dimensional Fourier power spectrum $P_1(k)$ of an image, where k is the wave number, was calculated. A large low-k peak, due to spatial nonuniformities in the illumination, was removed, and the power spectrum was azimuthally averaged. The resulting spectrum is peaked about a wave number k_c, and $\lambda_c = 2\pi/k_c$ can be taken as the characteristic length scale of the crack pattern. The spectra were asymmetric, with the skewness of the distribution being close to zero for the thinnest layers studied and increasing with depth. Figure 9 also shows the values of λ_c found in this way. The two methods of finding the length scale of the pattern are consistent.

As can be seen in Figs. 1 and 4, most polygons in the final pattern are four sided, and most crack junction angles are at 90°. Even non-four-sided polygons tend to have 90° corners; this is possible because the cracks which define their sides are curved. Examples of this can also be seen in Fig. 1. Figure 10 shows the distribution of n-sided polygons $P_2(n)$ averaged over all depths studied, for runs with the untreated substrate, the reduced friction substrate, and the treated substrate with added sand impurities. The distributions were essentially independent of depth over the range studied (0.13 mm $\leqslant d \leqslant$ 4.12 mm), except as noted below, and the distributions in the three cases are the same within the experimental uncertainties. With both the treated and untreated substrates (but without impurities), there is some indication of a drop in the fraction of three-sided polygons and a corresponding jump in the fraction of four-sided polygons as the depth increases above 1.5 mm. If this variation (which, although persistent, is within the statistical uncertainty of the data) is real, it is probably a result of cracks breaking off the corner of an existing polygon in the late stages of pattern formation, as described above. This process can turn, for example, a four-sided polygon into a three- or a five-sided polygon. This phenomenon is less common in thicker layers, and in runs with added impurities.

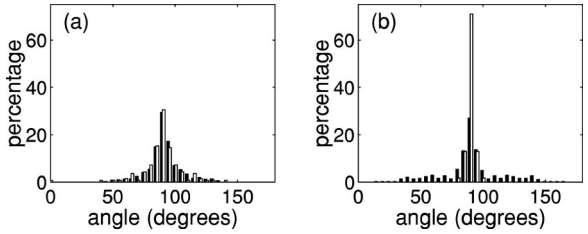

FIG. 11. The distribution of crack junction angles for selected runs. (a) Untreated substrate, no impurities. Solid bars: $d = 0.50 \pm 0.02$ mm; open bars: $d = 3.35 \pm 0.18$ mm. (b) Teflon-coated substrate, no impurities. Solid bars: $d = 0.80 \pm 0.05$ mm, open bars: $d = 2.70 \pm 0.08$ mm.

The distribution $P_3(\theta)$ of crack junction angles θ was sharply peaked at 90° for all runs. Sample distributions, using 5° bins for θ, are shown in Fig. 11. Figure 11(a) shows $P_3(\theta)$ for runs with the untreated substrate, for a relatively thin layer and a relatively thick layer. The distributions are essentially identical. In particular, the mean is 90° within the experimental uncertainties, and the width of the distribution does not change with depth. Figure 11(b) shows distributions for runs with the reduced-friction substrate. Again the mean is 90° for these runs, but in this case the distribution become much broader for thinner layers than for thicker layers. When sand was added to the layer, the mean remained at 90°, and again the distribution tended to broaden as d decreased. None of our runs had clear peaks at angles other than 90°; the broadening of the distribution for small d was due to a general spreading of the distribution and not to the emergence of peaks at, for example, 120°. Although symmetric triplets of cracks with junction angles of 120° were seen to nucleate in the early stages of drying, as discussed above, the number of such events was always too small to show up as a significant peak in the distribution functions, even in runs with sand added.

IV. DISCUSSION

Cracks develop in a drying layer when the shrinkage of the layer induces sufficient stress that the layer fractures. Our observations indicate that cracks initially appear by nucleation at a few points. When sand impurities were added to the layer, sand grains were frequent nucleation sites. Triplet junctions, at which three cracks meet with junction angles of 120°, are formed by such nucleations in the early stages of pattern development. At later times, however, cracks meet predominantly at 90° junctions. This is due to the fact that cracks propagate in the direction which most efficiently relieves the stress. Since the stress near a given crack is paral-

lel to its surface, other cracks will tend to approach and meet it at right angles.

The formation of crack patterns is strongly influenced by drying gradients, which in turn lead to stress gradients. Cracks tend to propagate in the direction of a dryness gradient. This is most obvious in the patterns produced in the directional drying experiments, but is also the cause of the laddering patterns observed in the isotropic experiments. The arching illustrated in Fig. 5 presumably also results from the interacting between the propagating crack and the local dryness or stress field.

Theories of crack-pattern formation [20,27] indicate that each generation of cracks should appear in the middle of existing fragments, leading to successive halvings of the length scale of the pattern. This follows from the fact that ideally the stress in a fragment of the drying layer will be a maximum midway between two cracks. A near-perfect halving of existing fragments, as in Fig. 8, was seen only rarely in our experiments. This is presumably due to unevenness in the local stress distributions, in turn resulting from nonuniform adhesion to the substrate and nonuniformities in the dryness and composition of the layer.

The spacing of the primary cracks in the directional drying experiments did not exhibit the halving effect either. Instead, the spacing that was quickly established near the beginning of the run propagated stably, as if we only observed the end point of the halving process. Even when sudden changes in stress were forced by propagating fronts over steps in the depth, spacing changes only occurred for rougher substrates.

The length scale of the final crack pattern in the isotropic experiments was found to be proportional to the layer depth, as shown in Fig. 9, with the constant of proportionality being largest for reduced friction between the layer and the substrate. This is in agreement with the experiments of Groisman and Kaplan [11], and also with the theoretical work of Kitsunezaki [23] under the assumption that the cracks develop as a result of a critical stress mechanism. This is easily understood. With reduced substrate adhesion, the stress in the layer will grow more slowly with distance away from an existing crack, and so a larger region is needed for the layer to reach the critical stress for fracture in that case.

The data in Fig. 10 show that the distributions of the number of sides of the polygons in the final pattern are essentially the same for the experimental conditions studied. The distribution of junction angles was sharply peaked at 90° in all runs. For experiments with the untreated substrate, there was no significant variation in the distribution of angles with depth, as indicated in Fig. 11(a). The standard deviation of the distribution was about 15° for all depths, and no peaks were observed at any other angles. With reduced bottom friction, both with and without added sand, the distribution broadened as the layer depth decreased, as indicated in Fig. 11(b). The standard deviation of the distribution increased from approximately 5° for layers 2.5 mm thick to 20° for layers 0.7 mm thick. Although nucleation of triple cracks was observed in the early stages of pattern formation, particularly with added sand, there was no sign of significant peaks in the distribution at angles other than 90°.

For comparison, Groisman and Kaplan [11] showed a distribution of junction angles for thick layers of a dried coffee-water mixture which has a mean of 93.1° and a standard deviation 8.0°. Groisman and Kaplan [11] observed a transition in the distribution of junction angles as the layer depth was decreased: for layers thinner than 4 mm, they observed a marked increase in the number of 120° junctions. In their thinnest layers, they found up to 30% 120° junctions. They explained this as being due to an increased likelihood of nucleation of cracks from inhomogeneities in the material when the layer thickness became roughly the same as the size of local inhomogeneities. While we do see a broadening of the distribution of angles when the substrate is coated with teflon, we observe no sharp transition down to layer depths of 0.5 mm, which is the size of the sand grains added to our mixture. We also see no evidence of a peak in the distribution at angles of 120°. It is likely that our alumina slurries were much more homogeneous than the coffee-water mixtures used in Ref. [11], but this does not explain the absence of an increase in the number of triplet junctions in thin layers with added sand.

The theoretical models of Refs. [20] and [22] predict that the appearance of the crack pattern should change as the amount of disorder in the system increases. With no sand added, our layers are very homogeneous and patterns are formed by cracks which propagate in straight lines and interact to form an array of predominantly four-sided polygons. These patterns are consistent with the model predictions in the case of weak disorder [20]. With sand added, and to some extent in thinner layers, the cracks tended to propagate shorter distances, and the patterns became closer to the type predicted for medium disorder. Thus our results provide a qualitative confirmation of the validity of the models.

V. CONCLUSIONS

Our isotropic drying experiments resulted in crack patterns which were similar in appearance to those predicted by theoretical models in the case of weak disorder. This is consistent with our expectation that the alumina-water mixtures used in our experiments were quite uniform in composition down to rather small length scales. The development of the crack patterns in our experiments did not proceed by a single well-characterized process. Initially, cracks nucleate at points. In layers with sand added, sand grains often serve as nucleation sites. The distribution of crack junction angles is strongly peaked at 90° for all experimental conditions studied. 120° triplet junctions can result from the symmetric nucleation of three cracks at a point, but most crack junctions form later in the development of the pattern when a propagating crack meets an older crack at 90°. We do not observe a dramatic increase in the fraction of triplet junctions nucleated as the layer becomes thinner, in contrast to the observations of Ref. [11]. Models predict that new cracks will form midway between existing cracks [20,27], leading to a halving of the pattern length scale with each successive generation of cracks. Although this process does sometimes occur, it is not predominant, at least partly because of nonuniformities in layer thickness, substrate adhesion, and drying. Other processes such as the laddering and arching described above are much more common. The laddering effect is most pronounced in the directional drying experiments. We found that the primary crack spacing in the directional experiments

did not show the halving effect either, but rather that the spacing tended to become established early and then propagate stably thereafter, even over sudden changes in depth. The spacing in the directional experiments depended on the substrate adhesion, but not on the speed of the front propagation.

In summary, we have performed an extensive experimental study of crack-pattern formation in both the isotropic and directional drying cases. Our results provide some confirmation of the predictions of theoretical models, but also underline the complexity of the pattern formation process in this system.

ACKNOWLEDGMENTS

This research was supported by NSERC of Canada. We acknowledge helpful discussions with N. Rivier, and P.-Y. Robin, and development work by Eamonn McKernan.

[1] J. Walker, Sci. Am. **255**, 204 (1986).
[2] M. P. Ryan and C. G. Sammis, Geol. Soc. Am. Bull. **89**, 1295 (1978); J. M. De Graaf and A. Aydun, *ibid.* **99**, 605 (1987); M. P. Ryan and C. G. Sammis, *ibid.* **89**, 1295 (1978); P. Budkewitsch and P.-Y. Robin, J. Volcanol. Geotherm. Res. **59**, 219 (1994).
[3] G. Müller, J. Geophys. Res. B **103**, 15 239 (1998).
[4] E. M. Kindle, J. Geol. **25**, 135 (1917).
[5] J. Q. Tompkins, Geol. Soc. Am. Bull. **76**, 1075 (1965); J. T. Neal, *ibid.* **77**, 1327 (1966); J. Q. Tompkins, *ibid.* **77**, 1331 (1966).
[6] L. B. Freund, *Dynamic Fracture Mechanics* (Cambridge University Press, New York, 1990).
[7] A. H. Lachenbruch, Geol. Soc. Am. Spec. Pap. **70**, (1962).
[8] Degussa Canada, Ltd.
[9] C. Allain and L. Limat, Phys. Rev. Lett. **74**, 2981 (1995).
[10] A. T. Skjeltorp and P. Meakin, Nature (London) **335**, 424 (1988).
[11] A. Groisman and E. Kaplan, Europhys. Lett. **25**, 415 (1994).
[12] J. Webb and T. Beddoe (unpublished).
[13] L. Pauchard, F. Parisse, and C. Allain, Phys. Rev. E **59**, 3737 (1999).
[14] W. Korneta, S. K. Mendiratta, and J. Menteiro, Phys. Rev. E **57**, 3142 (1998).
[15] J. V. Andersen, Phys. Rev. B **49**, 9981 (1994).
[16] J. V. Andersen, Y. Brechet, and H. J. Jensen, Europhys. Lett. **26**, 13 (1994).
[17] K.-t. Leung and J. V. Andersen, Europhys. Lett. **38**, 589 (1997).
[18] O. Morgenstern, I. M. Sokolov, and A. Blumen, Europhys. Lett. **22**, 487 (1993); J. Phys. A **26**, 4521 (1993).
[19] I. M. Sokolov, O. Morgenstern, and A. Blumen, Macromol. Symp. **81**, 235 (1994).
[20] T. Hornig, I. M. Sokolov, and A. Blumen, Phys. Rev. E **54**, 4293 (1996).
[21] U. A. Handge, I. M. Sokolov, and A. Blumen, Europhys. Lett. **40**, 275 (1997).
[22] K. M. Crosby and R. M. Bradley, Phys. Rev. E **55**, 6084 (1997).
[23] S. Kitsunezaki, Phys. Rev. E **60**, 6449 (1999).
[24] A. A. Griffiths, Philos. Trans. R. Soc. London, Ser. A **221**, 163 (1920).
[25] A. Yuse and M. Sano, Nature (London) **362**, 329 (1993); Physica D **108**, 365 (1998).
[26] S.-i. Sasa, K. Sekimoto, and H. Nakanishi, Phys. Rev. E **50**, R1733 (1994).
[27] T. S. Komatsu and S.-i. Sasa, Jpn. J. Appl. Phys. **36**, 391 (1997).
[28] Y. Hayakawa, Phys. Rev. E **49**, R1804 (1994).